

Dynamic Sparse Training via Balancing the Exploration-Exploitation Trade-off

Shaoyi Huang¹, Bowen Lei², Dongkuan Xu³, Hongwu Peng¹, Yue Sun⁴,
Mimi Xie⁵, Caiwen Ding¹

¹University of Connecticut, ²Texas A&M University, ³North Carolina State University,
⁴Lehigh University, ⁵University of Texas at San Antonio
{shaoyi.huang, hongwu.peng, caiwen.ding}@uconn.edu,
bowenlei@stat.tamu.edu, dxu27@ncsu.edu, yus516@lehigh.edu, mimi.xie@utsa.edu

Abstract

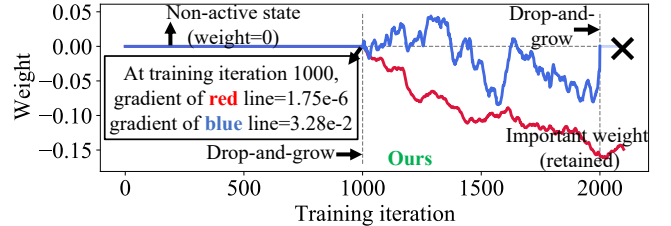
Over-parameterization of deep neural networks (DNNs) has shown high prediction accuracy for many applications. Although effective, the large number of parameters hinders its popularity on resource-limited devices and has an outsize environmental impact. Sparse training (using a fixed number of nonzero weights in each iteration) could significantly mitigate the training costs by reducing the model size. However, existing sparse training methods mainly use either random-based or greedy-based drop-and-grow strategies, resulting in local minimal and low accuracy. In this work, to assist explainable sparse training, we propose important weights Exploitation and coverage Exploration to characterize Dynamic Sparsity Training (DST-EE), and provide quantitative analysis of these two metrics. We further design an acquisition function and provide the theoretical guarantees for the proposed method and clarify its convergence property. Experimental results show that sparse models (up to 98% sparsity) obtained by our proposed method outperform the SOTA sparse training methods on a wide variety of deep learning tasks. On VGG-19 / CIFAR-100, ResNet-50 / CIFAR-10, ResNet-50 / CIFAR-100, our method has even higher accuracy than dense models. On ResNet-50 / ImageNet, the proposed method has up to 8.2% accuracy improvement compared to SOTA sparse training methods.

Introduction

Increasing deep neural networks (DNNs) model size has shown superior prediction accuracy in a variety of real-world scenarios (Goodfellow, Vinyals, and Saxe 2015; Brutzkus et al. 2018; Liu et al. 2021b). However, as model sizes continue to scale, a large amount of computation and heavy memory requirements prohibit the DNN training on resource-limited devices, as well as being environmentally unfriendly (Qi et al. 2021b; Peng et al. 2022; Qi et al. 2021a; Chen et al. 2021; Huang et al. 2022b; Peng et al. 2021; Huang et al. 2022a). A Google study showed that GPT-3 (Brown et al. 2020) (175 billion parameters) consumed 1,287 MWh of electricity during training and produced 552 tons of carbon emissions, equivalent to the emissions of a car for 120 years (Patterson et al. 2021). Fortunately, *sparse training could significantly mitigate the training costs by using a fixed and small number of nonzero weights in each iteration, while preserving the prediction accuracy for downstream tasks.*



(a) Non-active weights with small initial gradients are ignored in greedy-based weight growth methods (i.e., RigL, ITOP, ...)



(b) Non-active weights with small initial gradients could be retained and grown in proposed method.

Figure 1: Gradient-based weight growth methods vs. proposed method. (a) The red line shows the weight with a small gradient is ignored (not grown), while the blue line denotes that the weight with a large gradient is grown at iteration=1000. (b) Weight with a small gradient at iteration=1000 can be grown applying our method, and at training iteration = 2000 it is more important.

Two research trends on sparse training have attracted enormous popularity. One is *static mask*-based method (Lee, Ajanthan, and Torr 2019; Wang, Zhang, and Grosse 2020), where sparsification starts at initialization before training. Afterward, the sparse mask (a binary tensor corresponding to the weight tensor) is fixed. Such limited flexibility of subnetwork or mask selection leads to sub-optimal subnetworks with poor accuracy. To improve the flexibility, *dynamic mask training* has been proposed (Mocanu et al. 2018; Mostafa and Wang 2019; Evci et al. 2020; Liu et al. 2021b; Ma et al. 2021), where the sparse mask is periodically updated by drop-and-grow to search for better subnetworks with high accuracy, where in the drop process we deactivate a portion of weights from active states (nonzero) to non-active states (zero), vice versa for the growing process.

However, these methods mainly use either random-based or greedy-based growth strategies. The former one usu-

ally leads to lower accuracy while the latter one greedily searches for sparse masks with a local minimal in a short distance (He et al. 2022), resulting in limited weights coverage and thus a sub-optimal sparse model. As an illustration in Figure 1a using VGG-19/CIFAR-100, at one drop-and-grow stage (1,000th iteration), the gradient-based approach grows non-active weights with relatively large gradients but ignores small gradients. However, as training continues (e.g., at the 2,000th iteration), these non-active weights with small gradients will have large magnitude and hence are important to model accuracy (Renda, Frankle, and Carbin 2020; Zafrir et al. 2021). Therefore, they should be considered for the growth at the 1,000th iteration as shown in Figure 1b. In addition, more than 90% of non-active weights but important weights are ignored in 12 out of 16 convolutional layers.

To better preserve these non-active weights but important weights, we propose a novel weights Exploitation and coverage Exploration characterized Dynamic Sparse Training (DST-EE) to update the sparse mask and search for the “best possible” subnetwork. Different from existing greedy-based methods, which only exploit the current knowledge, we further explore and grow the weights that have never been covered in past training iterations, thus increasing the coverage of weights and avoiding the subnetwork searching process being trapped in a local optimum (Li et al. 2015). The contributions of the paper are summarized as follows:

- To assist explainable sparse training, we propose *important weights exploitation* and *weights coverage exploration* to characterize sparse training. We further provide the quantitative analysis of the strategy and show the advantage of the proposed method.
- We design an acquisition function for the growth process. We provide theoretical analysis for the proposed exploitation and exploration method and clarify the convergence property of the proposed sparse training method.
- Our proposed method does not need to train dense models throughout the training process, achieving up to 95% sparsity ratio and even higher accuracy than dense training, with same amount of iterations. Sparse models obtained by the proposed method outperform the SOTA sparse training methods.

On VGG-19 / CIFAR-100, ResNet-50 / CIFAR-10, ResNet-50 / CIFAR-100, our method has even higher accuracy than dense models. On ResNet-50 / ImageNet, the proposed method has up to 8.2% accuracy improvement. On graph neural network (GNN), our method outperforms prune-from-dense using ADMM algorithm (Zhang et al. 2021), achieving up to 23.3% higher link prediction accuracy.

Related Work

Static Mask Training. Single-Shot Network Pruning (SNIP) (Lee, Ajanthan, and Torr 2019) was the first to determine trainable and sparse sub-networks at initialization prior to training. It identified important weights and set the rest to zero with the aim of achieving comparable results. Motivated by SNIP (Lee, Ajanthan, and Torr 2019), several works have been inspired to explore training from scratch with the static

mask. GraSP (Wang, Zhang, and Grosse 2020) took the gradient norm as the criterion and considered the weights as less important if the removing of them would result in the least drop in the gradient norm. (de Jorge et al. 2021) observed that when a large portion of weights are pruned at initialization, the performance of both SNIP (Lee, Ajanthan, and Torr 2019) and GraSP (Wang, Zhang, and Grosse 2020) were worse than random pruning. Therefore, it used the saliency criteria (Mozer and Smolensky 1988) as the criterion in terms of weight importance and optimized the saliency after pruning with increased performance when sparsity is on high levels. SynFlow (Tanaka et al. 2020) proposed a gradient-based score pruning algorithm that preserved the total flow of weight importance through the network at initialization with avoiding layer collapse.

Dynamic Mask Training. Dynamic masks training adaptively updates mask tensors and provides more flexibility and hence higher accuracy. Sparse Evolutionary Training (SET) (Mocanu et al. 2018) removed least magnitude valued weights and randomly grow the corresponding number of weights back at the end of each training epoch. SNFS (Dettmers and Zettlemoyer 2019) utilized exponentially smoothed momentum to find the important weights and layers, and redistributed pruned weights based on the mean momentum magnitude per layer. RigL (Evci et al. 2020) updated the sparsity topology of the sparse network during training using the same magnitude-based weights dropping method while growing back the weights using top-k absolute largest gradients, achieving better accuracy than static mask training under same sparsity. However, the greedy-based growth policy leading to limited weights coverage, therefore a sub-optimal sparse model. ITOP (Liu et al. 2021b) discovered that the benefits of dynamic mask training come from its ability to consider across time all possible parameters. In addition, MEST (Yuan et al. 2021) employed a gradually decreasing drop and grow rate with a more relaxed range of parameters for growing. However, both ITOP and MEST keep the same drop-and-grow strategy as the existing works and have limited weights coverage. GaP (Ma et al. 2021) divides the DNN into several partitions, growing one partition at a time to dense and pruning the previous dense partition to sparse, with the aim of covering all weights. However, it requires more training time than traditional pruning methods, which limits its application on resources limited scenarios.

Methodology

The proposed dynamic sparse training (DST-EE) consists of two important components: (i) *important weights exploitation*, which exploits current knowledge (weights and gradients) to find the “best possible” sparse masks. Every ΔT iteration (ΔT is the sparse mask updating frequency), weights with high gradients will be grown, leading to high weights in the next iteration, therefore fast reducing the loss; (ii) *weights coverage exploration* in sparse training, which aims to explore uncovered weights and finally higher weights coverage, thus superior subnetworks to existing methods.

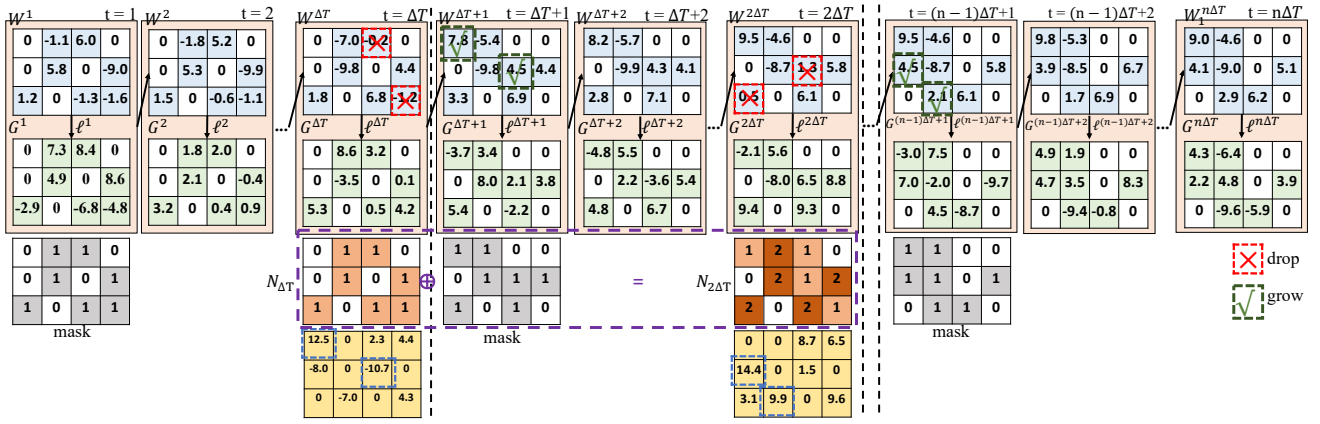


Figure 2: Sparse training data flow of proposed method.

Overview

We formalize the sparse training process of the proposed DST-EE as follows.

Initialization. We define a L -layer deep neural network with dense weight $\mathbf{W} = [\mathbf{W}_1, \mathbf{W}_2, \dots, \mathbf{W}_L]$. During the training process, the weight of i -th layer at t -th iteration is denoted by \mathbf{W}_i^t . We randomly initialize sparse weight tensor as $\mathbf{W}' = [\mathbf{W}'_1, \mathbf{W}'_2, \dots, \mathbf{W}'_L]$ with sparsity distribution of P using ERK (Mocanu et al. 2018) initialization. Each sparse weight tensor within a layer has a corresponding mask tensor (zero elements masked by 0 and other elements masked by 1) with the same size.

Training. We define zero elements in weight tensor as non-active weights and others as active weights. For each iteration, we only update the active weights.

Drop (deactivate): In addition, every ΔT iteration, we update the mask tensor, i.e., for i -th layer, we drop the k_i weights that are closest to zero (i.e., smallest positive weights and the largest negative weights), the dropped weights are denoted by $\text{ArgTopK}(\mathbf{W}'_i, k_i)$.

Grow (activate): We denote \mathbf{N}_i^t as the counter tensor that collects the occurrence frequency for each 1 mask. We initialize \mathbf{N}_i^t as a zero tensor with the same size as the corresponding weight tensor. Every ΔT iteration, the counter tensor is updated by adding the counter tensor with the existing mask tensor. We use \mathbf{S}_i^t to denote the importance score tensor in q -th mask update. We design the following acquisition function to compute the importance score tensor

$$\mathbf{S}_i^t = \left| \frac{\partial l(\mathbf{W}_i^t, \mathcal{X})}{\partial \mathbf{W}_i^t} \right| + c \frac{\ln t}{\mathbf{N}_i^t + \epsilon}, \quad t = q\Delta T, \quad i = 1, 2, \dots, L \quad (1)$$

where the first term $\left| \frac{\partial l(\mathbf{W}_i^t, \mathcal{X})}{\partial \mathbf{W}_i^t} \right|$ is the absolute gradient tensor of i -th layer at t -th iteration. $\partial l(\mathbf{W}_i^t, \mathcal{X})$ is the loss of i -th layer. \mathcal{X} is the input training data. In the second term $c \frac{\ln t}{\mathbf{N}_i^t + \epsilon}$, c is the coefficient to balance between the two terms and ϵ is a positive constant to make the remainder as nonzero. For each importance score tensor, we identify the k highest absolute values and select the indices. These corresponding mask

values with the same indices will be set to 1s. In the next iteration, we update the weights using the new mask tensor. In the whole process, we maintain that the newly activated weights are the same amount as the previously deactivated weights. We repeat the aforementioned iterations till the end of training. The details of our method are illustrated in Algorithm 1, where \cdot means tensor matrix multiplication.

Algorithm 1: DST-EE

Input: a L -layer network f with dense weight $\mathbf{W} = [\mathbf{W}_1, \mathbf{W}_2, \dots, \mathbf{W}_L]$; sparsity distribution: $P = P_1, P_2, \dots, P_L$; total number of training iterations T_{end} .
Set \mathcal{X} as the training dataset; ΔT as the update frequency; α as the learning rate; k_1, k_2, \dots, k_L are variables denoting the number of weights dropped every ΔT iterations; $\mathbf{M}_1, \mathbf{M}_2, \dots, \mathbf{M}_L$ are the sparse masks. $\mathbf{S}_1, \mathbf{S}_2, \dots, \mathbf{S}_L$ are the importance score tensors.
Output: a L -layer sparse network with sparsity distribution P .
 $\mathbf{W}' = [\mathbf{W}'_1, \mathbf{W}'_2, \dots, \mathbf{W}'_L] \leftarrow \text{sparsify } \mathbf{W}_1, \mathbf{W}_2, \dots, \mathbf{W}_L \text{ with } P$
 $\mathbf{N}_i^t \leftarrow \mathbf{M}_i$
for each training iteration t **do**
 Loss $\delta_t \leftarrow f(x_t, \mathbf{W}')$, $x_t \in \mathcal{X}$
 if $t \pmod{\Delta T} = 0$ and $t < T_{end}$ **then**
 for $0 < i < L + 1$ **do**
 $\mathbf{W}'_i \leftarrow \text{ArgDrop}(\mathbf{W}'_i, \text{ArgTopK}(\mathbf{W}'_i, k_i))$
 $\mathbf{S}_i = \nabla(\mathbf{W}'_i) \delta_t + c * \frac{\ln t}{\mathbf{N}_i^t + \epsilon}$
 $\mathbf{W}'_i \leftarrow \text{ArgGrow}(\mathbf{W}'_i, \text{ArgTopK}(\mathbf{S}_i \cdot (\mathbf{M}_i == 0), k_i))$
 end for
 $\mathbf{N}_i^t \leftarrow \mathbf{N}_i^t + \mathbf{M}_i$
 else
 $\mathbf{W}'_i \leftarrow \mathbf{W}'_i - \alpha \nabla(\mathbf{W}'_i) \delta_t$
 end if
end for
return Trained model

Figure 2 shows the training data flow of one layer using the proposed method. We use \mathbf{W}^t and \mathbf{G}^t to denote the weight and gradient tensor, respectively. n is the total number of rounds of mask updates. l^t is the loss to compute the gradient tensor. In the first iteration of each ΔT , the weight tensor has a corresponding binary mask tensor, where zero elements are masked by 0 in the mask tensor and other elements are masked by 1. \mathbf{N}_i is the counting tensor, indicating the number of non-zero occurrences in previous mask updates.

Important Weights Exploitation in Sparse Training

In proposed sparse training, we exploit current knowledge (weights and gradients) and define the exploitation score to help decide the mask with the highest accuracy. More specifically, we define the exploitation score $\mathbf{S}_{\text{exploit}}$ in q -th mask update as the first item of Eq. (1), i.e., $\mathbf{S}_{\text{exploit}} = \left| \frac{\partial l(\mathbf{W}_i^t, \mathcal{X})}{\partial \mathbf{W}_i^t} \right|$, $t = q\Delta T$, $i = 1, 2, \dots, L$.

We further propose an evaluation metric to quantify the degree of exploitation for weight growth. With high degree of exploitation, the policy will find a model with local minimal with large loss reduction in a short time. Therefore, a growth policy is designed to have a high exploitation degree if it leads to a fast reduction in losses in the next iteration.

To formulate the evaluation metric, we denote $\mathbf{W} = [w_1^{(1,1)}, w_1^{(1,2)}, \dots, w_1^{(m_1, n_1)}, \dots, w_j^{(p,q)}, \dots, w_L^{(m_L, n_L)}]$ as weight of a model, where $w_j^{(p,q)}$ denotes the weight element in the p -th row and q -th column of j -th layer in the model. j -th layer has m_j rows and n_j columns. We further define $\mathbf{W}_{j pq, -j pq} = [0, \dots, 0, w_j^{(p,q)}, 0, \dots, 0]$ with same size of \mathbf{W} . The degree of exploitation is denoted as $\Delta \mathcal{L}_g^{j pq}$ when the weight element in the p -th row and q -th column of j -th layer is grown in sparse mask update iteration, then

$$\Delta \mathcal{L}_g^{j pq} = \mathcal{L}(\mathbf{W}) - \mathcal{L}(\mathbf{W} + \mathbf{W}_{j pq, -j pq}). \quad (2)$$

To generalize, we use $\Delta \mathcal{L}_g$ to denote the degree of exploitation of the model if k weights with indices of I_1, I_2, \dots, I_k are grown, then

$$\Delta \mathcal{L}_g = \mathcal{L}(\mathbf{W}) - \mathcal{L}(\mathbf{W} + \sum_{n=1}^k \mathbf{W}_{I_n, -I_n}). \quad (3)$$

Weights Coverage Exploration in Sparse Training

Besides exploitation, we simultaneously prefer to choose masks that have never been explored so the model will not be stuck in a bad local optimum. We define our exploration score $\mathbf{S}_{\text{explor}}$ as the second item in Eq. (1), i.e., $\mathbf{S}_{\text{explor}} = \frac{\ln t}{\mathbf{N}_i^t + \epsilon}$, $t = q\Delta T$, $i = 1, 2, \dots, L$, where \mathbf{N}_i^t is a counter tensor that collects the active (nonzero) occurrence frequency of each element. If an element with an active (nonzero) occurrence frequency of zero, it will have a corresponding higher exploration score than explored elements, thus being grown.

Applying exploration brings the benefit of increased diversity which is a popular measurement referring to differences among the explored sparse masks (Črepinšek, Liu, and Mernik 2013). High diversity usually leads to better search performance (high accuracy), while a lack of diversity often results in stagnation (low accuracy). Numerous theoretical and empirical works have been trying to understand how diversity influence the control over exploration and exploitation (Črepinšek, Liu, and Mernik 2013; Raghavan et al. 2018; Xu and Zhang 2014).

We also propose an evaluation metric to quantify the degree of exploration for weight growth. Assume $\mathbf{B} = [b_1^{(1,1)}, b_1^{(1,2)}, \dots, b_1^{(m_1, n_1)}, \dots, b_j^{(p,q)}, \dots, b_L^{(m_L, n_L)}]$ is a binary

vector to denote if the corresponding parameter in \mathbf{W} is explored (1) or not (0) throughout the process of sparse training.

We define $R = \frac{\sum_{j=1}^L \sum_{p=1}^{m_j} \sum_{q=1}^{n_j} b_j^{(p,q)}}{\sum_{j=1}^L m_j \times n_j}$ as exploration degree.

Balancing the Exploitation-Exploration Trade-off

The mask tensor search task is challenging in sparse training. Firstly, the mask search task is a high-dimensional problem due to a large number of weights in DNNs. Secondly, the search space has many local minima and saddle points (Han et al. 2016; Xie, Liang, and Song 2017) because of the non-convex loss function of DNNs (Han et al. 2016; Xie, Liang, and Song 2017). Therefore, the mask tensor search process is easily trapped in a bad local optimal because of its low global exploration efficiency (Li et al. 2015) or needs a longer time to fully explore the loss landscape.

A better balance between exploration and exploitation can encourage search algorithms to better understand the loss landscape and help the sparse model escape from the bad local optima. The importance and challenges of balancing the exploration and exploitation tradeoff have been emphasized in many studies (Črepinšek, Liu, and Mernik 2013; Wilson et al. 2021). However, they have not gained enough attention in sparse training. Therefore, there is a strong need to better control the balance and we propose to consider both the exploration and exploitation scores when choosing the mask. And our importance score in Eq. (1) combines the two scores and overcome the limitations of previous work.

Theoretical Justification

Inspired by (Ma et al. 2021), we provide the convergence guarantee for our algorithm. We use $F(W) = \mathbb{E}_{x \sim \mathcal{X}} f(x; W)$ to denote the loss function for our sparse training where \mathcal{X} is the data generation distribution. We use $\nabla f(x; W)$ and $\nabla F(W)$ to denote the complete stochastic and accurate gradients in terms of W , respectively. For each round (ΔT iterations), we update the mask and use $M^{[q]}$ to denote the mask selected for the q -th round, $W^{[q]}$ to denote the model weights after $q - 1$ round training. Aligned with Ma et al. (2021), we make the following assumptions:

Assumption 1. (Smoothness). We assume the objective function $F(W)$ is partition-wise L -smooth, i.e.,

$$\|\nabla F(W + h) - \nabla F(W)\| \leq L\|h\|,$$

where h is in the same size with W .

Assumption 2. (Gradient noise) We assume for any t and q that

$$\begin{aligned} \mathbb{E}[\nabla f(x_t^{(q)}; W)] &= \nabla F(W), \\ \mathbb{E}[\|\nabla f(x_t^{(q)}; W) - \nabla F(W)\|^2] &\leq \sigma^2 \end{aligned}$$

where $\sigma > 0$ and $x_t^{(q)}$ is independent of each other for any t and q .

Assumption 3. (Mask-incurred error) We assume that

$$\|W_t^{(q)} \odot M^{(q)} - W_t^{(q)}\|^2 \leq \tau^2 \|W_t^{(q)}\|^2$$

where $\tau \in [0, 1)$.

Datasets	#Epochs	CIFAR-10			CIFAR-100		
Sparsity ratio		90%	95%	98%	90%	95%	98%
VGG-19(Dense)	160	93.85 \pm 0.05			73.43 \pm 0.08		
SNIP (Lee, Ajanthan, and Torr 2019)	160	93.63	93.43	92.05	72.84	71.83	58.46
GraSP (Wang, Zhang, and Grosse 2020)	160	93.30	93.04	92.19	71.95	71.23	68.90
SynFlow (Tanaka et al. 2020)	160	93.35	93.45	92.24	71.77	71.72	70.94
STR (Kusupati et al. 2020)	160	93.73	93.27	92.21	71.93	71.14	69.89
SIS (Verma and Pesquet 2021)	160	93.99	93.31	93.16	72.06	71.85	71.17
DeepR (Bellec et al. 2018)	160	90.81	89.59	86.77	66.83	63.46	59.58
SET (Mocanu et al. 2018)	160	92.46	91.73	89.18	72.36	69.81	65.94
RigL (Evci et al. 2020)	160	93.38 \pm 0.11	93.06 \pm 0.09	91.98 \pm 0.09	73.13 \pm 0.28	72.14 \pm 0.15	69.82 \pm 0.09
DST-EE (Ours)	160	93.84 \pm 0.09	93.53 \pm 0.08	92.55 \pm 0.08	74.27 \pm 0.18	73.15 \pm 0.12	70.80 \pm 0.15
DST-EE (Ours)	250	94.13 \pm 0.09	93.67 \pm 0.09	92.95 \pm 0.03	74.76 \pm 0.07	73.91 \pm 0.13	71.51 \pm 0.10
ResNet-50(Dense)	160	94.75 \pm 0.01			78.23 \pm 0.18		
SNIP (Lee, Ajanthan, and Torr 2019)	160	92.65	90.86	87.21	73.14	69.25	58.43
GraSP (Wang, Zhang, and Grosse 2020)	160	92.47	91.32	88.77	73.28	70.29	62.12
SynFlow (Tanaka et al. 2020)	160	92.49	91.22	88.82	73.37	70.37	62.17
STR (Kusupati et al. 2020)	160	92.59	91.35	88.75	73.45	70.45	62.34
SIS (Verma and Pesquet 2021)	160	92.81	91.69	90.11	73.81	70.62	62.75
RigL (Evci et al. 2020)	160	94.45 \pm 0.43	93.86 \pm 0.25	93.26 \pm 0.22	76.50 \pm 0.33	76.03 \pm 0.34	75.06 \pm 0.27
DST-EE (Ours)	160	94.96 \pm 0.23	94.72 \pm 0.18	94.20 \pm 0.08	78.15 \pm 0.17	77.54 \pm 0.25	75.68 \pm 0.11
DST-EE (Ours)	250	95.01 \pm 0.16	94.92 \pm 0.22	94.53 \pm 0.03	79.16 \pm 0.06	78.66 \pm 0.31	76.38 \pm 0.10

Table 1: Test accuracy of sparse VGG-19 and ResNet-50 on CIFAR-10/CIFAR-100 datasets. The results reported with (mean \pm std) are run with three different random seeds. The highest test accuracy scores are marked in bold. DST-EE denotes our proposed method.

Methods	Epochs	Training FLOPS (\times e18)	Inference FLOPS (\times e9)	Top-1 Acc (%)	Training FLOPS (\times e18)	Inference FLOPS (\times e9)	Top-1 Acc (%)
Dense	100	3.2	8.2	76.8 \pm 0.09	3.2	8.2	76.8 \pm 0.09
Sparsity ratio	-	80%			90%		
SNIP (Lee, Ajanthan, and Torr 2019)	-	0.23 \times	0.23 \times	-	0.10 \times	0.10 \times	-
GraSP (Wang, Zhang, and Grosse 2020)	150	0.23 \times	0.23 \times	72.1	0.10 \times	0.10 \times	68.1
DeepR (Bellec et al. 2018)	-	n/a	n/a	71.7	n/a	n/a	70.2
SNFS (Dettmers and Zettlemoyer 2019)	-	n/a	n/a	73.8	n/a	n/a	72.3
DSR (Mostafa and Wang 2019)	-	0.40 \times	0.40 \times	73.3	0.30 \times	0.30 \times	71.6
SET (Mocanu et al. 2018)	-	0.23 \times	0.23 \times	72.9 \pm 0.39	0.10 \times	0.10 \times	69.6 \pm 0.23
RigL (Evci et al. 2020)	100	0.23 \times	0.23 \times	74.6 \pm 0.06	0.10 \times	0.10 \times	72.0 \pm 0.05
MEST (Yuan et al. 2021)	100	0.23 \times	0.23 \times	75.39	0.10 \times	0.10 \times	72.58
RigL-ITOP (Liu et al. 2021b)	100	0.42 \times	0.42 \times	75.84 \pm 0.05	0.25 \times	0.24 \times	73.82 \pm 0.08
DST-EE(Ours)	100	0.23 \times	0.42 \times	76.25 \pm 0.09	0.10 \times	0.24 \times	75.3 \pm 0.06

Table 2: Performance of sparse ResNet-50 models on ImageNet dataset. The results reported with (mean \pm std) are run with three different random seeds.

Under Assumptions 1-3, we establish Proposition 1 to show the loss decrease in each round. Then, we get Proposition 2 to show that our sparse training algorithm converges to the stationary model at rate $O(1/\sqrt{Q})$ under the proper learning rate. The proof is included in the Appendix.

Proposition 1. *Under assumptions 1-3, it holds for each q that*

$$\mathbb{E}[F(W^{[q+1]})] \leq \mathbb{E}[F(W^{[q]})] - \frac{\alpha \Delta T}{12} \mathbb{E}[\|\nabla F(W^{[q]})\|^2] + \frac{\alpha^2 L \sigma^2 \Delta T^2}{2} + \frac{2\alpha L^2 \tau^2 \Delta T^2}{3} \mathbb{E}[\|W^{[q]}\|^2]. \quad (4)$$

where α is the learning rate.

For Proposition 1, we make the following remark

Remark 1. *In each round of our DST-EE, the loss value can decrease by $\frac{\alpha \Delta T}{12} \mathbb{E}[\|\nabla F(W^{[q]})\|^2]$. However, two additional errors will be added and slow the convergence, which is due to the stochastic gradient and inexact search of the mask.*

Proposition 2. *If the learning rate $\alpha = 1/(16L\Delta T\sqrt{Q})$, the sparse models generated by our algorithm after Q mask updates will converge as follows:*

$$\begin{aligned} & \frac{1}{Q} \sum_{q=1}^Q \mathbb{E}[\|\nabla F(W^{[q]} \odot M^{[q]})\|^2] \\ &= O\left(\frac{G}{\sqrt{Q}} + \frac{\tau^2}{Q} \sum_{q=1}^Q \mathbb{E}[\|W^{[q]}\|^2]\right) \end{aligned} \quad (5)$$

where G is a constant depending on the stochastic gradient noise and the model initialization.

In regard to Proposition 2, we make the following remarks:

Remark 2. *During dense training, we do not have error introduced by the mask selected and have $\tau^2 = 0$. As shown in Eq. (5), we will have $\mathbb{E}(\|\nabla F(W^{[Q]} \odot M^{[Q]})\|) \rightarrow 0$, indicating that DST-EE will converge to a stationary point as Q increases to infinity.*

Remark 3. During sparse training, the error τ^2 introduced by the mask selected will directly influence the model’s performance. Our algorithm can improve mask search through a better balance between exploitation and exploration, which leads to a more accurate model.

Experimental Results

Experimental Setup

We evaluate VGG-19 (Simonyan and Zisserman 2014) and ResNet-50 (He et al. 2016) on CIFAR-10/CIFAR-100 and evaluate ResNet-50 on ImageNet (Deng et al. 2009). The model training and evaluation are performed with CUDA 11.1 on 8 Quadro RTX6000 GPUs and Intel(R) Xeon(R) Gold 6244 @ 3.60GHz CPU. For CIFAR-10/CIFAR-100, we set the total number of training epochs as 160, while for ImageNet we set the total number of training epochs as 100. We use a cosine annealing learning rate scheduler with an SGD optimizer. For CIFAR-10/100, we use a batch size of 128 and set the initial learning rate to 0.1. For ImageNet, we use a batch size of 128. We use the same sparsity initialization method ERK in the state-of-the-art sparse training method such as RigL (Evci et al. 2020) and ITOP (Liu et al. 2021b). To further validate the generalizability of the proposed method, we conduct experiments on graph neural network for link prediction tasks on ia-email (Rossi and Ahmed 2015) (87,274 nodes and 1,148,072 edges) and wiki-talk (Cunningham and Craig 2019) (1,140,149 nodes and 7,833,140 edges) datasets.

Experimental Results

CIFAR-10/CIFAR-100. The results of CIFAR-10/100 are shown in Table 1. We compare our method with SOTA on VGG-19 and ResNet-50 models at sparsity of 90%, 95%, and 98%. To demonstrate the effectiveness of the proposed method, we compare it with three types of methods (i.e., pruning-at-initialization (SNIP, GraSP, SynFlow), dense-to-sparse training (STR, SIS), and dynamic sparse training (DeepR, SET, RigL)) from top to bottom. The results of baselines are obtained from the GraNet (Liu et al. 2021a) paper. Overall, both pruning-at-initialization and dense to sparse methods have higher accuracy than dynamic sparse training (except for RigL (using ITOP (Liu et al. 2021b) setting)). Among the various sparsities, the proposed method achieves the highest accuracy for both VGG-19 and ResNet-50. Using typical training time (total training epochs is 160), there is almost no accuracy loss compared to the dense model at sparsity of 90% on both CIFAR-10 and CIFAR-100. On both VGG-19 and ResNet-50, the proposed method has the highest accuracy compared with SOTA sparse training methods at different sparsity on both CIFAR-10 and CIFAR-100 datasets. For VGG-19, our method has up to 3.3%, 4.6% and 6.7% increase in accuracy on CIFAR-10 and up to 11.1%, 15.3% and 18.8% higher performance in accuracy on CIFAR-100, at sparsities 90%, 95% and 98%, respectively. For ResNet-50, our proposed method has accuracy improvement than RigL with the same training epochs. More specifically, on CIFAR-10, our method has 0.51, 0.86, 0.94 higher accuracy at sparsities 90%, 95%, 98%, respectively. On CIFAR-100,

the accuracy improvements of the proposed method compared to the SOTA sparse training method are 2.2%, 2.0%, 0.83% at sparsities of 90%, 95%, and 98%, respectively.

ImageNet. Table 2 shows the top-1 accuracy results, training and inference FLOPS on ResNet50 / ImageNet. We use the dense training model as our baseline. For other baselines, we select SNIP (Lee, Ajanthan, and Torr 2019) and GraSP (Wang, Zhang, and Grosse 2020) as the static mask training baselines while adopting DeepR (Bellec et al. 2018), SNFS (Dettmers and Zettlemoyer 2019), DSR (Mostafa and Wang 2019), SET (Mocanu et al. 2018), RigL (Evci et al. 2020), MEST (Yuan et al. 2021), RigL-ITOP (Liu et al. 2021b) as the dynamic mask training baselines as shown in Table 2. Compared to static mask training baselines, our proposed method has up to 5.8% and 10.6% increase in accuracy. For the dynamic mask training baselines, RigL is the recently popular baseline, compared with which the proposed method has 2.2% and 3.7% higher Top-1 accuracy at sparsity ratios of 80% and 90%, respectively. For the other two better baselines of sparse training, MEST and RigL-ITOP, our method has 1.1% and 0.5% higher accuracy at a sparsity ratio of 0.8, and 3.7% and 1.48% accuracy improvement at a sparsity ratio of 0.9, respectively.

Methods	Epochs	Sparsity ratio 80%	Sparsity ratio 90%	Sparsity ratio 98%
Dense	-		79.72	
Prune-from-dense	60	79.05	78.34	78.08
DST-EE (ours)	50	79.28	79.13	78.58

Table 3: Results on the graph neural network for link prediction tasks on wiki-talk (Cunningham and Craig 2019).

Methods	Epochs	Sparsity ratio 80%	Sparsity ratio 90%	Sparsity ratio 98%
Dense	-		83.47	
Prune-from-dense	60	83.19	82.95	67.18
DST-EE (ours)	50	83.77	83.29	82.82

Table 4: Results on the graph neural network for link prediction tasks on ia-email (Rossi and Ahmed 2015).

Graph Neural Network. Experimental results of sparse training of graph neural network on wiki-talk (Cunningham and Craig 2019) and ia-email (Rossi and Ahmed 2015) for link prediction task are shown in Table 3 and Table 4, respectively. We apply the proposed method to the two fully connected layers with uniform sparsity ratios at different sparsity levels, which are 80%, 90%, and 98%. We report the prediction accuracy of the best model searched in 50 training epochs. We compare our method with both the dense model and the best sparse model pruned from the dense model using ADMM algorithm (Zhang et al. 2021). The prune-from-dense models are trained for 60 epochs in total, which of 20 pretraining epochs, 20 reweighted training epochs, and 20 retraining epochs after pruning. Experimental results show that at a sparsity of 0.8, our sparse training method has even better accuracy than the dense model. The proposed method has accuracy improvement compared with prune-from-dense on both datasets using even fewer training epochs. On wiki-talk (Cunningham and Craig 2019), our method has 0.29%,

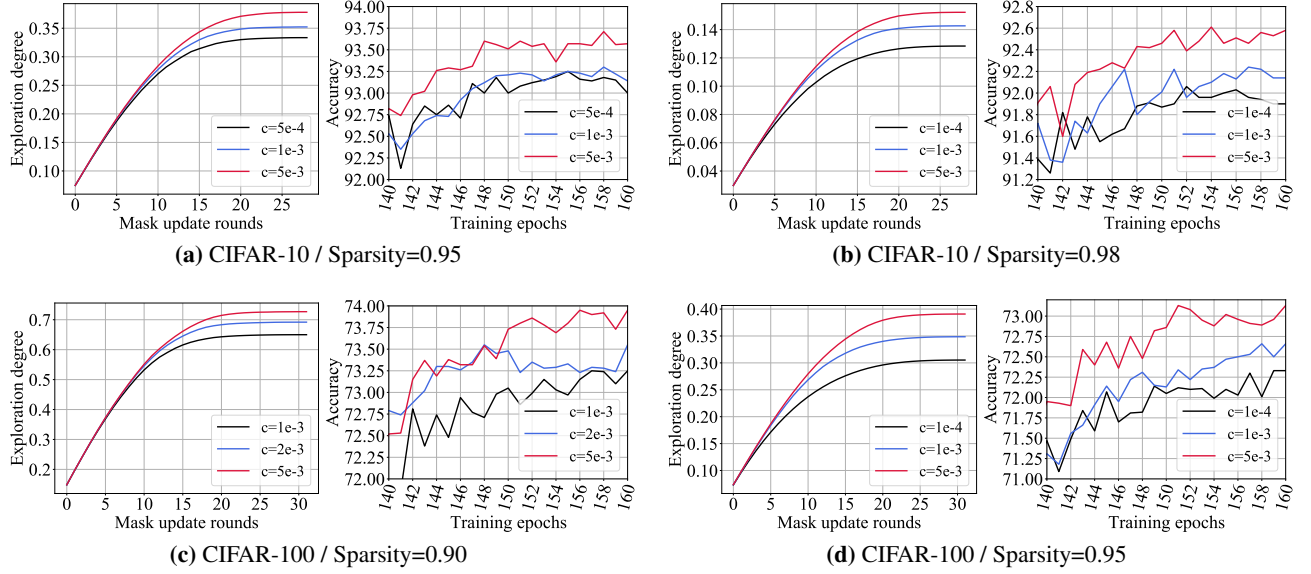


Figure 3: The figure shows the relation of exploration degrees and test accuracy on CIFAR-10 with sparsity of 0.95 and 0.98, and CIFAR-100 with sparsity of 0.90 and 0.95.

1.0% and 0.64% higher accuracy than prune-from-dense using ADMM algorithm at sparsity ratios of 80%, 90% and 98%, respectively. On ia-email (Rossi and Ahmed 2015), the proposed method has up to 23.3% accuracy improvement than prune-from-dense at a sparsity ratio of 98%.

Ablation Studies

Effects of Extended Training Time. We test our method using extended training time (total number of training epochs is 250) on VGG-19/ResNet-50 models and CIFAR-10/CIFAR-100 datasets. On CIFAR-10 (90% sparsity ratio), and CIFAR-100 (90% and 95% sparsity ratios), there is no decrease in the accuracy of both models compared to dense models. For VGG-19, there is only 0.19% and 0.96% accuracy degradation on CIFAR-10 at 95% and 98% sparsity ratios compared to the dense model, while on CIFAR-100, DST-EE outperforms SOTA methods by at least 1.7%, 2.0% and 2.5% at 90%, 95%, and 98% sparsity ratios, respectively. For ResNet-50, there is no accuracy drop at 90% and 95% sparsity ratios on both datasets. On CIFAR-10, it has 8.4%, 6.5%, 6.4%, 6.5%, 4.9% and 1.4% higher accuracy performance at 98% sparsity ratio compared to SNIP (Lee, Ajanthan, and Torr 2019), GraSP (Wang, Zhang, and Grosse 2020), SynFlow (Tanaka et al. 2020), STR (Kusupati et al. 2020), SIS (Verma and Pesquet 2021) and RigL (Evci et al. 2020), respectively. On CIFAR-100, DST-EE has at least 1.8% and at most 30.7% accuracy improvement compared to SOTA.

Effects of Different Exploration Degrees on Test Accuracy. The study of different exploration degrees on VGG-19, CIFAR-10 / CIFAR-100 datasets are shown in Figure 3. We investigate the effect of coefficients on exploration degree and the effect of coefficients on test accuracy. Then, we unveil the relation between exploration degree and test accuracy. The left subfigure in Figure 3a shows the different exploration

degree curves generated using different tradeoff coefficients on CIFAR-100 with a sparsity of 0.95. The x-axis is the mask update rounds and the y-axis is the exploration degree. We could see the larger c , the higher degree of exploration of the sparse model. The right subfigure in Figure 3a illustrates the test accuracy curves for different coefficients, the x-axis is the number of training epochs while the y-axis is the test accuracy. Within the coefficient range, the larger c , the higher test accuracy. The combination of these two subfigures unveils the observation that the higher the exploration degree or higher weights coverage, the higher the test accuracy score. Similar observations are shown in Figure 3b, Figure 3c and Figure 3d, which validate our methods.

Conclusion

In this paper, we propose important weights exploitation and coverage exploration-driven growth strategy to characterize and assist explainable sparse training, update the sparse masks and search for the “best possible” subnetwork. We provide theoretical analysis for the proposed exploitation and exploration method and clarify its convergence property. We further provide the quantitative analysis of the strategy and show the advantage of the proposed method. We design the acquisition function to evaluate the importance of non-active weights for growth and grow the weights with top-k highest importance scores, considering the balance between exploitation and exploration. Extensive experiments on various deep learning tasks on both convolutional neural networks and graph neural networks show the advantage of DST-EE over existing sparse training methods. We conduct experiments to quantitatively analyze the effects of exploration degree. The observations validate the proposed method, i.e., our method could achieve a higher exploration degree and thus a higher test accuracy compared to greedy-based methods.

References

- Bellec, G.; Kappel, D.; Maass, W.; and Legenstein, R. 2018. Deep rewiring: Training very sparse deep networks. *International Conference on Learning Representations (ICLR)*.
- Brown, T. B.; Mann, B. P.; Ryder, N.; Subbiah, M.; Kaplan, J.; Dhariwal, P.; Neelakantan, A.; Shyam, P.; Sastry, G.; Askell, A.; Agarwal, S.; Herbert-Voss, A.; Krüger, G.; Henighan, T.; Child, R.; Ramesh, A.; Ziegler, D. M.; Wu, J.; Winter, C.; Hesse, C.; Chen, M.; Sigler, E. J.; Litwin, M.; Gray, S.; Chess, B.; Clark, J.; Berner, C.; McCandlish, S.; Radford, A.; Sutskever, I.; and Amodei, D. 2020. Language Models are Few-Shot Learners.
- Brutzkus, A.; Globerson, A.; Malach, E.; and Shalev-Shwartz, S. 2018. SGD Learns Over-parameterized Networks that Provably Generalize on Linearly Separable Data. In *International Conference on Learning Representations*.
- Chen, S.; Huang, S.; Pandey, S.; Li, B.; Gao, G. R.; Zheng, L.; Ding, C.; and Liu, H. 2021. ET: re-thinking self-attention for transformer models on GPUs. In *Proceedings of the International Conference for High Performance Computing, Networking, Storage and Analysis*, 1–18.
- Črepinšek, M.; Liu, S.-H.; and Mernik, M. 2013. Exploration and exploitation in evolutionary algorithms: A survey. *ACM computing surveys (CSUR)*, 45(3): 1–33.
- Cunningham, S.; and Craig, D. 2019. Creator Governance in Social Media Entertainment. *Social Media + Society*, 5.
- de Jorge, P.; Sanyal, A.; Behl, H. S.; Torr, P. H.; Rogez, G.; and Dokania, P. K. 2021. Progressive skeletonization: Trimming more fat from a network at initialization. *ICLR*.
- Deng, J.; Dong, W.; Socher, R.; Li, L.-J.; Li, K.; and Fei-Fei, L. 2009. Imagenet: A large-scale hierarchical image database. In *2009 IEEE conference on computer vision and pattern recognition*, 248–255. Ieee.
- Dettmers, T.; and Zettlemoyer, L. 2019. Sparse networks from scratch: Faster training without losing performance. *arXiv preprint arXiv:1907.04840*.
- Evci, U.; Gale, T.; Menick, J.; Castro, P. S.; and Elsen, E. 2020. Rigging the lottery: Making all tickets winners. In *International Conference on Machine Learning*, 2943–2952. PMLR.
- Goodfellow, I. J.; Vinyals, O.; and Saxe, A. M. 2015. Qualitatively characterizing neural network optimization problems. *International Conference on Learning Representations*.
- Han, S.; Pool, J.; Narang, S.; Mao, H.; Gong, E.; Tang, S.; Elsen, E.; Vajda, P.; Paluri, M.; Tran, J.; et al. 2016. Dsd: Dense-sparse-dense training for deep neural networks. *arXiv preprint arXiv:1607.04381*.
- He, K.; Zhang, X.; Ren, S.; and Sun, J. 2016. Identity mappings in deep residual networks. In *European conference on computer vision*, 630–645. Springer.
- He, Z.; Xie, Z.; Zhu, Q.; and Qin, Z. 2022. Sparse Double Descent: Where Network Pruning Aggravates Overfitting. In *International Conference on Machine Learning*, 8635–8659. PMLR.
- Huang, S.; Liu, N.; Liang, Y.; Peng, H.; Li, H.; Xu, D.; Xie, M.; and Ding, C. 2022a. An automatic and efficient bert pruning for edge ai systems. In *2022 23rd International Symposium on Quality Electronic Design (ISQED)*, 1–6. IEEE.
- Huang, S.; Xu, D.; Yen, I.; Wang, Y.; Chang, S.-E.; Li, B.; Chen, S.; Xie, M.; Rajasekaran, S.; Liu, H.; et al. 2022b. Sparse Progressive Distillation: Resolving Overfitting under Pretrain-and-Finetune Paradigm. In *Proceedings of the 60th Annual Meeting of the Association for Computational Linguistics (Volume 1: Long Papers)*, 190–200.
- Kusupati, A.; Ramanujan, V.; Somani, R.; Wortsman, M.; Jain, P.; Kakade, S.; and Farhadi, A. 2020. Soft threshold weight reparameterization for learnable sparsity. In *International Conference on Machine Learning*, 5544–5555. PMLR.
- Lee, N.; Ajanthan, T.; and Torr, P. 2019. SNIP: SINGLE-SHOT NETWORK PRUNING BASED ON CONNECTION SENSITIVITY. In *International Conference on Learning Representations*.
- Li, Z.; Wang, W.; Yan, Y.; and Li, Z. 2015. PS-ABC: A hybrid algorithm based on particle swarm and artificial bee colony for high-dimensional optimization problems. *Expert Systems with Applications*, 42(22): 8881–8895.
- Liu, S.; Chen, T.; Chen, X.; Atashgahi, Z.; Yin, L.; Kou, H.; Shen, L.; Pechenizkiy, M.; Wang, Z.; and Mocanu, D. C. 2021a. Sparse training via boosting pruning plasticity with neuroregeneration. *Advances in Neural Information Processing Systems*, 34: 9908–9922.
- Liu, S.; Yin, L.; Mocanu, D. C.; and Pechenizkiy, M. 2021b. Do we actually need dense over-parameterization? in-time over-parameterization in sparse training. In *International Conference on Machine Learning*, 6989–7000. PMLR.
- Ma, X.; Qin, M.; Sun, F.; Hou, Z.; Yuan, K.; Xu, Y.; Wang, Y.; Chen, Y.-K.; Jin, R.; and Xie, Y. 2021. Effective Model Sparsification by Scheduled Grow-and-Prune Methods. In *International Conference on Learning Representations*.
- Mocanu, D. C.; Mocanu, E.; Stone, P.; Nguyen, P. H.; Gibescu, M.; and Liotta, A. 2018. Scalable training of artificial neural networks with adaptive sparse connectivity inspired by network science. *Nature communications*, 9(1): 1–12.
- Mostafa, H.; and Wang, X. 2019. Parameter efficient training of deep convolutional neural networks by dynamic sparse reparameterization. In *International Conference on Machine Learning*, 4646–4655. PMLR.
- Mozer, M. C.; and Smolensky, P. 1988. Skeletonization: A technique for trimming the fat from a network via relevance assessment. *Advances in neural information processing systems*, 1.
- Patterson, D.; Gonzalez, J.; Le, Q.; Liang, C.; Munguia, L.-M.; Rothchild, D.; So, D.; Texier, M.; and Dean, J. 2021. Carbon emissions and large neural network training. *arXiv preprint arXiv:2104.10350*.
- Peng, H.; Huang, S.; Chen, S.; Li, B.; Geng, T.; Li, A.; Jiang, W.; Wen, W.; Bi, J.; Liu, H.; et al. 2022. A length adaptive algorithm-hardware co-design of transformer on fpga through sparse attention and dynamic pipelining. In *Proceedings of*

- the 59th ACM/IEEE Design Automation Conference, 1135–1140.
- Peng, H.; Huang, S.; Geng, T.; Li, A.; Jiang, W.; Liu, H.; Wang, S.; and Ding, C. 2021. Accelerating transformer-based deep learning models on fpgas using column balanced block pruning. In *2021 22nd International Symposium on Quality Electronic Design (ISQED)*, 142–148. IEEE.
- Qi, P.; Sha, E. H.-M.; Zhuge, Q.; Peng, H.; Huang, S.; Kong, Z.; Song, Y.; and Li, B. 2021a. Accelerating framework of transformer by hardware design and model compression co-optimization. In *2021 IEEE/ACM International Conference On Computer Aided Design (ICCAD)*, 1–9. IEEE.
- Qi, P.; Song, Y.; Peng, H.; Huang, S.; Zhuge, Q.; and Sha, E. H.-M. 2021b. Accommodating transformer onto fpga: Coupling the balanced model compression and fpga-implementation optimization. In *Proceedings of the 2021 on Great Lakes Symposium on VLSI*, 163–168.
- Raghavan, M.; Slivkins, A.; Wortman, J. V.; and Wu, Z. S. 2018. The externalities of exploration and how data diversity helps exploitation. In *Conference on Learning Theory*, 1724–1738. PMLR.
- Renda, A.; Frankle, J.; and Carbin, M. 2020. Comparing rewinding and fine-tuning in neural network pruning. *arXiv preprint arXiv:2003.02389*.
- Rossi, R. A.; and Ahmed, N. 2015. The Network Data Repository with Interactive Graph Analytics and Visualization. In *AAAI*.
- Simonyan, K.; and Zisserman, A. 2014. Very deep convolutional networks for large-scale image recognition. *arXiv preprint arXiv:1409.1556*.
- Tanaka, H.; Kunin, D.; Yamins, D. L.; and Ganguli, S. 2020. Pruning neural networks without any data by iteratively conserving synaptic flow. *Advances in Neural Information Processing Systems*, 33: 6377–6389.
- Verma, S.; and Pesquet, J.-C. 2021. Sparsifying networks via subdifferential inclusion. In *International Conference on Machine Learning*, 10542–10552. PMLR.
- Wang, C.; Zhang, G.; and Grosse, R. 2020. Picking winning tickets before training by preserving gradient flow. *n International Conference on Learning Representations*.
- Wilson, R. C.; Bonawitz, E.; Costa, V. D.; and Ebitz, R. B. 2021. Balancing exploration and exploitation with information and randomization. *Current opinion in behavioral sciences*, 38: 49–56.
- Xie, B.; Liang, Y.; and Song, L. 2017. Diverse neural network learns true target functions. In *Artificial Intelligence and Statistics*, 1216–1224. PMLR.
- Xu, J.; and Zhang, J. 2014. Exploration-exploitation tradeoffs in metaheuristics: Survey and analysis. In *Proceedings of the 33rd Chinese control conference*, 8633–8638. IEEE.
- Yuan, G.; Ma, X.; Niu, W.; Li, Z.; Kong, Z.; Liu, N.; Gong, Y.; Zhan, Z.; He, C.; Jin, Q.; et al. 2021. MEST: Accurate and Fast Memory-Economic Sparse Training Framework on the Edge. *Advances in Neural Information Processing Systems*, 34.
- Zafir, O.; Larey, A.; Boudoukh, G.; Shen, H.; and Wasserblat, M. 2021. Prune once for all: Sparse pre-trained language models. *arXiv preprint arXiv:2111.05754*.
- Zhang, T.; Ye, S.; Feng, X.; Ma, X.; Zhang, K.; Li, Z.; Tang, J.; Liu, S.; Lin, X.; Liu, Y.; et al. 2021. Structadmm: Achieving ultrahigh efficiency in structured pruning for dnns. *IEEE Transactions on Neural Networks and Learning Systems*, 33(5): 2259–2273.